



Feasibility of Cathodic Protection in Grouted Post Tensioned Tendons - Exploratory Model Calculations.

Jacob Bumgardner
Alberto Sagüés
University of South Florida,
4202 E. Fowler Ave., Tampa, Florida, 33620
United States

ABSTRACT

Recent corrosion related failures of grouted post tensioned tendons, even after the introduction of improved grouts, have led to renewed interest in supplemental or backup means of corrosion control for these systems. A finite element model is presented to explore feasibility of impressed current protection of strand in grouted tendons. The model examines polarization evolution as function of service time and includes consideration of anode placement and size, grout porosity, pore water alkalinity, electrochemical species diffusivity and applied voltage on the polarization efficacy and durability of such a system. The exploratory model projections suggested that, within the context of the design parameters assumed, an impressed current cathodic protection system installed internally into a grouted duct for the purpose of cathodic protection of steel tensioning strand may be feasible for the case of initially passive steel.

Key words: COMSOL Multiphysics, Impressed Current Cathodic Protection, Post-Tensioning Strands, FDOT

INTRODUCTION

Corrosion of steel in concrete and cementitious media is one major issue facing American infrastructure.^{1,2,3} High strength strand in bridge post tensioning (PT) tendons have recently experienced unexpected corrosion related failures even after the introduction of improved cementitious grouts intended to prevent voids and other corrosion-inducing deficiencies⁴. There is uncertainty as to the precise corrosion mechanism so alternative avenues of corrosion control are being explored with renewed interest, given the critical structural nature of PT components. Among those alternatives, including such techniques as cement mineral admixtures, alternative duct fills such as grease, and external polarization methods, Impressed Current Cathodic Protection (ICCP) is receiving attention as an approach meriting further consideration. Conceptually, ICCP involves applying an external electrical current to the strands by way of an anode running parallel to the reinforcement inside the tendon duct, to polarize the steel in the cathodic direction, thus promoting the stability of the passive regime, or lowering the rate of corrosion had it already began. Assuming that an anode wire could be introduced practically before grouting, and fitted with periodic insulation spacers to avoid short circuits with the strands, several electrochemical issues would need assessment to ascertain whether the system could

operate in a beneficial and efficient manner. Concerns to resolve would include (but not be limited to) acidification of the grout, possible Hydrogen evolution which could lead to strand embrittlement,^{5,6} and whether current delivery to the strand assembly would be sufficient to ensure an adequate level of cathodic protection (CP).

In order to explore means of assessing the viability of using such an impressed current cathodic protection system in post-tensioning systems, a 2D finite element conceptual physical model was created to simulate the electrochemical behavior of the system. The model simulates a six strand duct filled with grout where the central location that would have contained another strand has been replaced with a wire type CP anode. The goal of this approach is to create an integral model to assess the viability of such a system, creating a framework to evaluate issues such as the effect of anode placement and size, grout porosity, pore water alkalinity, electrochemical species diffusivity and applied voltage on the polarization efficacy and durability of such a system.

In the initial realization presented here, the model studies polarization behavior of the electrodes, tertiary current distribution, oxygen transport, ionic species distribution and migration due to electric fields and faradaic reactions, current density and its distribution on the cathodes (the strands), calcium hydroxide dissolution from the hydrated cement matrix and acidification around the anode due to hydroxide consumption. In particular, the model assesses whether an ICCP system could deliver a sufficient level of protective current and adequate polarization to the entire surface of the reinforcing strands without reaching levels that would generate Hydrogen, (with associated risk of hydrogen embrittlement^{5,6}) and without acidifying the concrete to an extent that would damage the anode or lower its ability to provide current.

The calculations here are limited to the relatively easier to achieve case of the polarization of initially passive steel. More demanding cases, such as polarization of steel after active corrosion starts should be evaluated subsequently if the present results prove to be encouraging.

PROCEDURE

Geometric Arrangement

The model was built in COMSOL Multiphysics® platform. The model (Figure 1) simulates the inside of a notional six strand duct filled with grout where the central location, that would have contained another strand, has been replaced with a wire type CP anode. The grout domain was 6 in (0.152 m) in diameter; each of the strands was of ½ in (0.0123 m) nominal diameter and with the strand center located 2 in (0.0508 m) from the duct center.

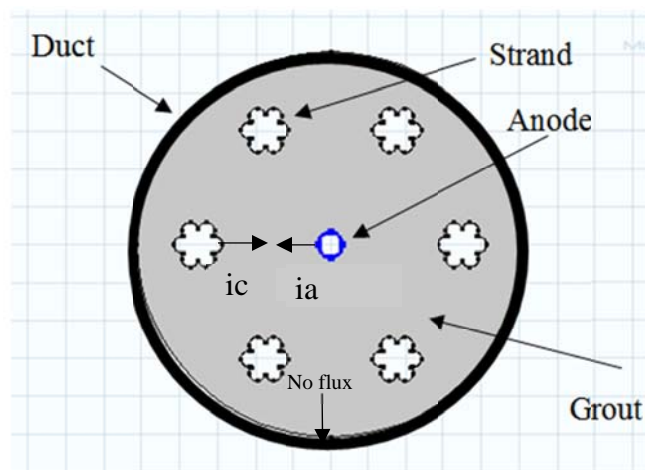


Figure 1: Schematic Drawing of the Model Space

The model included a detailed representation of the metallic perimeter of a 7-wire strand, to assess to which extent steel polarization may reach into the receded line of contact between wires. The centrally located anode was $\frac{1}{4}$ in (0.0061 m) in diameter and was envisioned as being made of a mixed metal/metal oxide material of the type commonly used for CP of reinforcing steel.

Assumptions and Ruling Equations

The pore water of cementitious grout is a complex and highly alkaline solution⁴. For the purposes of our calculations we have assumed the concrete pores contain a solution of Ca^{2+} , Na^+ , OH^- , O_2 , and water, and that a substantial quantity of $Ca(OH)_2$ is present in the hydrated cement matrix. The calcium hydroxide is assumed to rapidly achieve equilibrium with the pore water calcium and Hydroxide ions so the equilibrium reaction given in Eq. 1 applies



The model treats the reaction equilibrium between solid calcium hydroxide in concrete and the dissolved species in pore water based on kinetic theory as outlined in Peelen et al.⁷. The grout is treated for simplicity as if it were a homogeneous medium with properties representative of the average composition and effective porosity and pore interconnectivity of the actual system. The Faradaic reactions assumed to apply to the major carrier of ionic current in the system is oxygen reduction, which proceeds via the reactions,



at the cathodes, and at the anode.



A tertiary current distribution⁸ has been simulated by introducing a current at the anode and cathodes as a function of an externally applied voltage, the potential differences across the electrochemical interfaces (polarizations) and the concentrations of the relevant species. Eq. 4 gives the inward current density^A (i_c) at the cathodes and Eq. 5 gives the inward current density at the anodes (i_a).

$$i_a = \frac{OH}{CoOH} * i_{oa} * 10^{\frac{E_{exta}-V+E_{oa}}{Ba}} \quad (4)$$

$$i_c = -\frac{O}{Co} * i_{oc} * 10^{\frac{V-E_{oc}}{Bc}} \quad (5)$$

where O is the concentration of oxygen, present as molecular O_2 in the grout, in mol/l , OH is the concentration of hydroxide in mol/l , Co is the initial oxygen concentration in mol/l , and CoOH is the initial hydroxide concentration in mol/l . V is the potential in the grout at a point immediately next to the electrode interface^B in Volts. E_o , i_o , and B are electrochemical constants for the anode abstracted from Bartholemew et al.³ by idealized Tafel extrapolation and for the cathodes from Dugarte et al.⁹, and E_{exta} is the potential applied externally by a notional rectifier to the system (potential of the metal in the anode minus that of the steel) in Volts. Parameter values are listed in Table 1. This system of equations treats the cathode as the ground and therefore the potential in the grout projected by the finite element

^A That is, the conventional current density coming from the outside into the grout domain. At a net anodic interface that current density is of positive sign.

^B As measured by an SCE electrode with the tip placed on that point, and with the metallic contact connected to the *positive* terminal of an ideal voltmeter and the other terminal connected to the metal. This convention is the opposite of that in typical half-cell potential measurements but is used here to match the potential definition scheme of the finite element computation package.

package and the applied potential at the anode is given relative to the Cathode potential. In addition to the above, there was a small passive dissolution current $i_p=10^{-4} A/m^2$ assumed for the steel¹⁰.

In order to keep the molar (mass) and electrical charge flow consistent the oxygen reduction reaction proceeds at the rate of the current flow through the interface such that

$$J_i = i_i * \frac{1}{nF} \quad (6)$$

where J_i is the molar flux of species i in $mol/(m^2 s)$, F is Faraday's constant in C/mol , and n is the number of electrons exchanged per reaction in Eqs. (2) and (3).

Transport of charged species is governed by the Nernst-Planck equation⁸:

$$J = -zFD \left[\nabla c + \frac{Fz}{RT} (\nabla \phi) \right] \quad (7)$$

where D is the diffusivity of that species in m^2/s , ∇c is the gradient of the homogenized concentration of the species mol/m^3 , $\nabla \phi$ is the gradient of the grout potential in V/m , and J is the charge flux associated for that species in A/m^2 , and the electroneutrality condition.

$$\sum(z_j c_j) = 0 \quad (8)$$

Since oxygen is uncharged and therefore not affected by electric fields its behavior is modeled by Fick's second law.

$$\frac{\partial c}{\partial t} = D \nabla^2 c \quad (9)$$

where D is the diffusivity for oxygen, assumed to be constant throughout the simulation domain. We follow the treatment by Ukrainczyk et al.¹¹ where detailed description of the system of equations governing treatment of charged species flow through the model can be found.

The parameters used in the model for the concentration and behavior of ionic species in grout are presented in Table 1. The values were tentatively selected from literature sources^{7,12-17} for the purpose of these exploratory calculations, with the understanding that a wide range of alternative values may be applicable as well.

The model outputs a time dependent solution over a period of a simulated design lifetime of 100 years. Output of the calculations includes electric potential and the concentrations of the chemical species modeled in the grout domain over the time period examined. From these values current densities, species flux, and dissolution rates can be calculated as secondary outputs with the intention of evaluating the durability and efficacy of the modeled system.

The main operating parameter and material property examined were the externally applied potential and the grout resistivity, with attention to their effect on achievable protective current density, polarization on the strand assembly, and compositional changes of the grout and pore water in the neighborhood of the anode as an indicator of possible detrimental aging effects. The resistivity in the following is meant as that calculated from the effective ionic mobilities and concentrations of the species in the system in the *initial* condition (year zero), as it would be measured by an AC device in the usual manner. It is cautioned that as the system ages, under the influence of the DC regime the ionic concentrations vary in time and space, and the local and global relationships between electric field and current depart from those found initially, so potential drops along the electrolyte no longer can be simply obtained with input from the initial resistivity value. The base case modeled a hydroxide diffusivity of $1 \cdot 10^{-10} m^2/s$, which yielded an AC grout resistivity of 80 ohm-m, and an applied polarization voltage of 1 Volt. Variations of those parameters were evaluated as well.

Table 1: Electrochemical Properties of Concrete and Model Inputs

Parameter	Illustrative range/value in comparable literature treatments ^{3,7,9,12-17}	Chosen values*	Description
Porosity (assumed saturated)	1.0E-01 – 1.9E-01	1.12E-01	Portion of the matrix that is pore space
Density (kg/m ³)	2.4E+03	2.4E+03	Nominal density
D OH eff (m ² /s)	1E-11 – 2E-10**	8E-11 - 4E-10***	Effective hydroxide diffusivity
D Na eff (m ² /s)	0.16E-12 – 1.33E-11	2.00E-12	Effective sodium diffusivity
D K eff (m ² /s)	0.24E-12 – 1.96E-11	5.00E-12	Effective potassium diffusivity
D Ca eff (m ² /s)	7.90E-12	7.90E-12	Effective calcium diffusivity
D O eff (m ² /s)	1E-08 – 3E-08	3.00E-08	Effective oxygen diffusivity
Homogenized Pore K (mol/m ³)	8.0E+01 – 4.50E+02	-	Grout potassium concentration, model bundles Potassium and Sodium content
Homogenized Pore Na (mol/m ³)	2.5E01 – 1E03	3.55E+02	Grout Sodium concentration, assumed primary counter ion to Hydroxide
Homogenized Pore OH (mol/m ³)	1.05E+02 – 1.50E+03	3.55+02****	Effective hydroxide concentration given pH 13.5
Homogenized Pore Ca (mol/m ³)	1E+00	1.40E-02	Calcium concentration such that calcium is in kinetic equilibrium with hydroxide
Homogenized Solid Ca(OH) ₂ (mol/ m ³)	3.5 E03	3.5E03	Calcium hydroxide concentration in the bulk
Homogenized initial oxygen content (mol/ m ³)	0.3	0.3	Nominal initial oxygen content
ioa (A/m ²)	Linked to Eoa choice	2.00E-05	Nominal polarization parameter, anode ³
Eoa (V SCE)	Linked to ioa choice	0	Nominal polarization parameter, anode ³
Ba (V/Decade)	1.5E-01 – 5E-01	0.15	Nominal polarization parameter, anode ³
ioc (A/m ²)	Linked to Eoc choice	2.00E-05	Nominal polarization parameter, steel ⁹
Eoc (V SCE)	Linked to Eoc choice	0	Nominal polarization parameter, steel ⁹
Bc (V/Decade)	1.0E-01 – 4.0E-01	0.138	Nominal polarization parameter, steel ⁹
Ip (A/m ²)	1E-4	1E-4	Passive anodic current at steel
* Species contents for these exploratory calculations are representative of comparable simulations for concrete. Values for grout may vary, including greater Ca(OH) ₂ content than the effectively conservative choice used here.			
** For Portland cement, dependent upon water to cement ratio			
*** The range describes a grout with an AC resistivity ^C from 10 ohm - m to 200 ohm-m			
**** Equivalent to a pH of 13.5 and stated porosity.			

RESULTS

Current Distribution

One measure of ICCP system efficacy is current density impressed on the cathode. Current densities typical of systems that offer cathodic protection in concrete and similar media fall into the range of $0.2\mu A/(cm^2)$ to $2\mu A/(cm^2)$ ¹⁸. For this reason, projected current densities within this range will be considered in the following to be at a sufficient level to keep the metal protected under normal conditions and thereby prevent or significantly delay the initiation and propagation of corrosion.

The model projects that the magnitude of the current density perpendicular to the electrode's surface decays toward a near steady state over a period of ten years, after which it stabilizes until the calcium hydroxide at the anode is completely depleted. Thus a conservative estimate of the system's performance prior to the depletion of calcium hydroxide at the anode would use that lower stabilization value of the current density. As it will be shown, calculations indicate a time to complete calcium

^C That is, the resistivity that corresponds to the effective concentrations and mobilities of the ionic species and that would be measured using an alternating current method whereby no net ionic flux occurs during the measurement.

hydroxide dissolution at the anode greater than the design lifetime of the system, and so, that conservative estimate has been used as the indicator of system performance.

In our base case ($D_{OH\ eff} = 1 \times 10^{-10} \text{ m}^2/\text{s}$), 1.5 Volts applied potential) the lowest inward current density at the cathode during the stabilization period was approximately $0.88 \text{ uA}/(\text{cm}^2)$, which is within the target range assumed above for cathodic protection. The distribution of current density predicted by the base case parameter set is shown in Figure 2. By varying the hydroxide diffusivity as a proxy for variations in pore network interconnectivity we simulated the behavior of a range of grout resistivities from $10 \text{ Ohm}\cdot\text{m}$ to $200 \text{ Ohm}\cdot\text{m}$. Furthermore calculations were run over a range of applied voltages from 0.5V to 2V, with results shown in Figure 3 for a system age of 10 years.

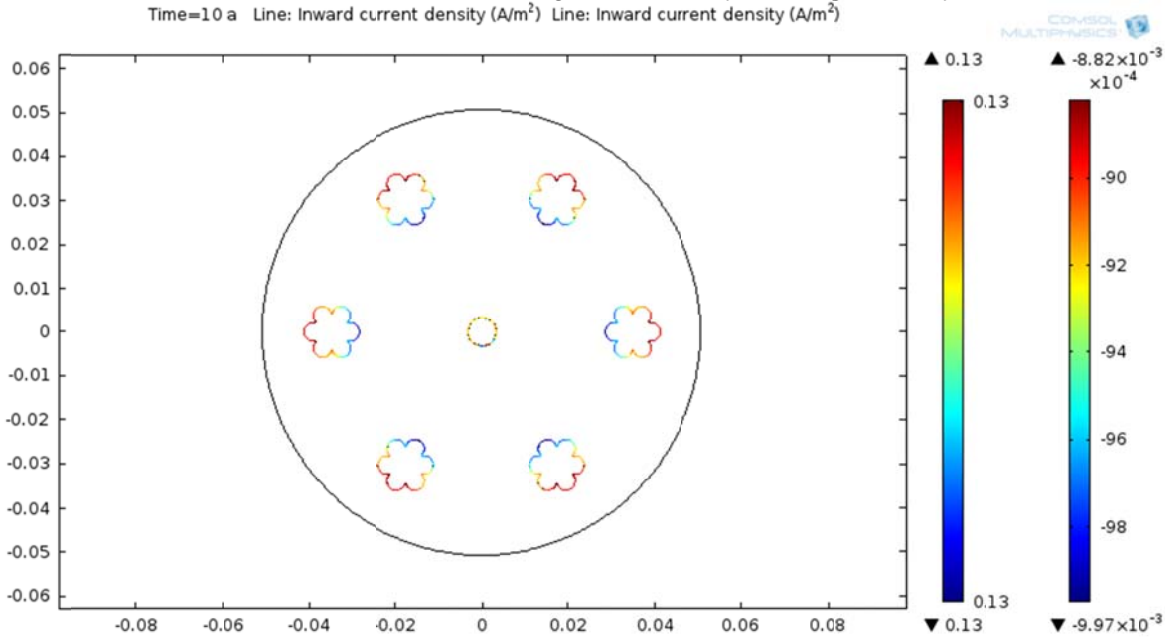


Figure 2: Current Distribution of the Base Case Model Parameter Set. Anode and Cathode Current Density Shown in Left and Right Legend Respectively. Legend is in A/m^2 .

In general, applied voltages higher than about 1 V yielded appreciable projected current densities, suggesting that usable operation may be obtained without excessive applied voltage needs. It is noted that the magnitude of the current density on the strand is, as expected, lower on the back side facing away from the anode. However, the effect is not very strong and appreciable current reaches even into the receded line of contact between wires on the back side. The minimum value corresponding to that location has been used as a performance indicator. Figure 3 shows the results for that minimum.

It can be observed in the 0.5, 0.75 and 1 Volt curves in Figure 3 that below a certain simulated grout resistivity the system current is relatively stable. This is consistent with a system current that is limited by polarization and charge transfer efficiency of the electrodes. Above a given grout resistivity the projected system current tends to be inversely proportional the grout resistivity. The latter behavior is consistent with mass transfer limited systems. Between the mass transfer limited and electrochemically limited regions the model projects a curved transition zone with mixed limitation.

The observed dependence on parameters in the mass transfer limited region may be abstracted via a power law relationship (indicated by the trend lines) of minimum cathodic current density ($\text{A}/(\text{cm}^2)$) versus grout resistivity ($\Omega \cdot \text{m}$) for a given applied voltage, such that a characteristic curve may be proposed of the form:

$$i_{c\ min} = (a p^{-1}) \quad (10)$$

where a represents an applied voltage dependent intercept for an idealized power law extrapolation of the log of the projected minimum current density versus the log of the assumed grout resistivity. This

relationship may be a useful future tool in designing CP system optimal operation for the period after stabilization is reached; performance monitoring and adjustment may be necessary during early operation.

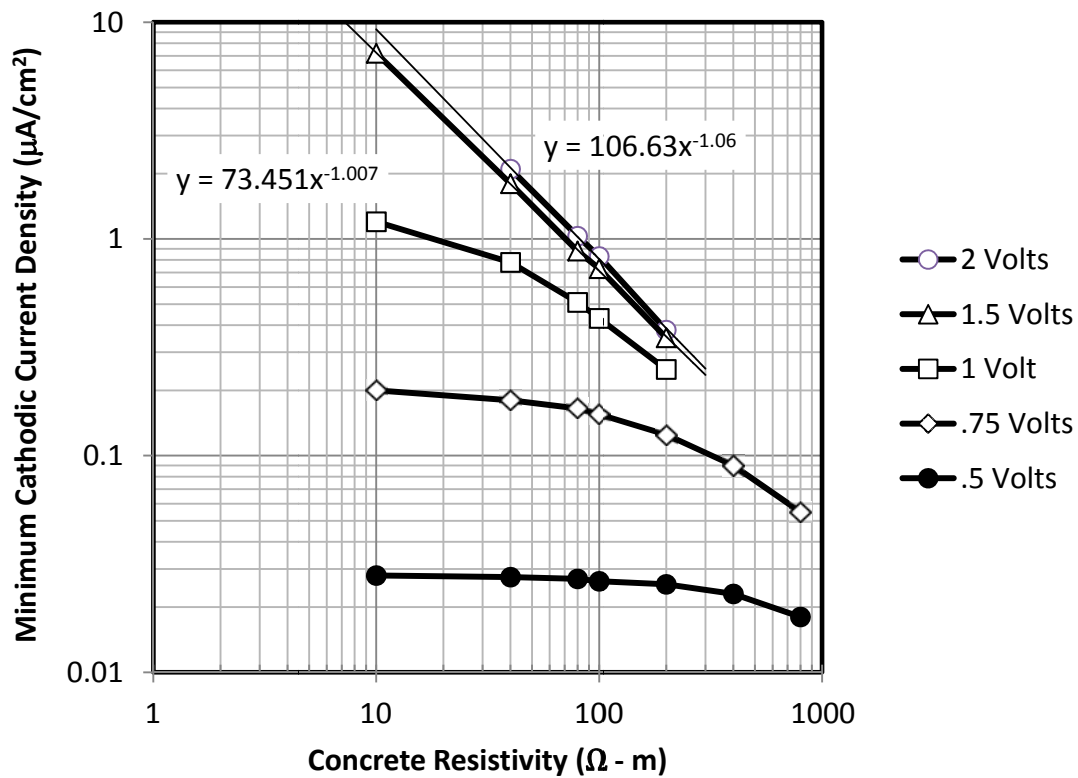


Figure 3: Minimum Cathodic Current Density vs Grout Resistivity (Initial Value, See Text) for a Range of Applied Voltages. System age 10 years.

Cathodic Polarization Achieved

Another measure of ICCP system efficacy is the potential shift of the steel (with respect to the unpolarized condition) under cathodic protection. Typical potential shift values required for cathodic protection are on the order of one Tafel slope¹⁹. In this case this would be represented by a potential shift $\sim 0.15V$ (somewhat more conservative than the commonly used 100 mV criterion²⁰) for ICCP system efficacy. With no polarizing current the potential of the steel under the present parameter choices is $\sim 100\text{ mV}^D$. Under the base case parameter set (as described in the current distribution section) the model projected a steel potential cathodic shift $\sim 250\text{ mV}$ relative to the unpolarized case, meeting the above criterion. Figure 4 shows the potential profile of the grout relative to the steel strand of the base case parameter set after the stabilization period of the system. Note that much of the ohmic potential drop occurs near the anode, as expected given its narrow diameter. Further investigations will include examination of the projected effect of depolarization of the steel once the ionic system has stabilized, and consideration of polarization of actively corroding steel as well as the passive steel condition examined here.

^D Note that this potential would be -100 mV when conventionally measured. The same distinction applies to all other potential reported as a model output.

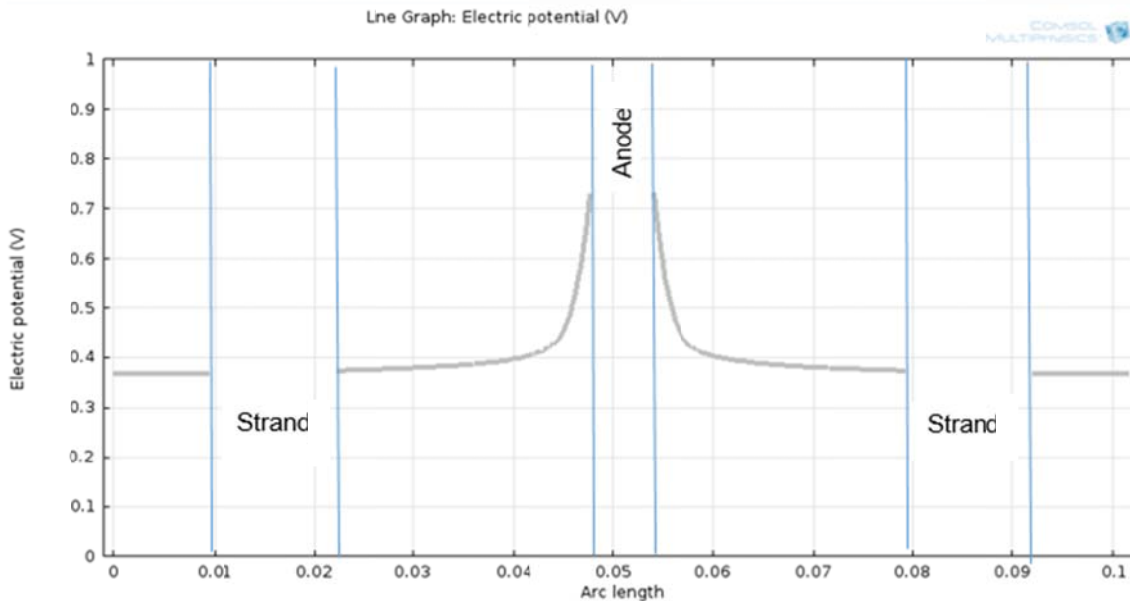


Figure 4: Potential Distribution Profile of the Grout With Respect to the Cathode of the Base Case Parameter Set After the Stabilization Period (~>10 Y Age). Note Potentials are Given on Sign Convention Opposite of Usual (See Footnotes 2 And 4).

Hydroxide – Calcium Hydroxide Reactions

At the anode, hydroxide is consumed via the reaction shown in Formula 3. The consumption of hydroxide ions at the anode creates a hydroxide concentration gradient between the anode and the cathodes where hydroxide is being generated as shown in Formula 2. The result of this is the pore water near the anode is depleted in hydroxide ions while the pore water near the cathodes is enriched. This issue is of interest in determining the extent to which concrete may deteriorate near the anode and how that may limit the achievable current density. Figure 5 shows the stabilized period grout hydroxide ion concentration profile projected by the base case parameter set, and Figure 6 shows the stabilized period pore solution pH distribution projected by the base case parameter set.

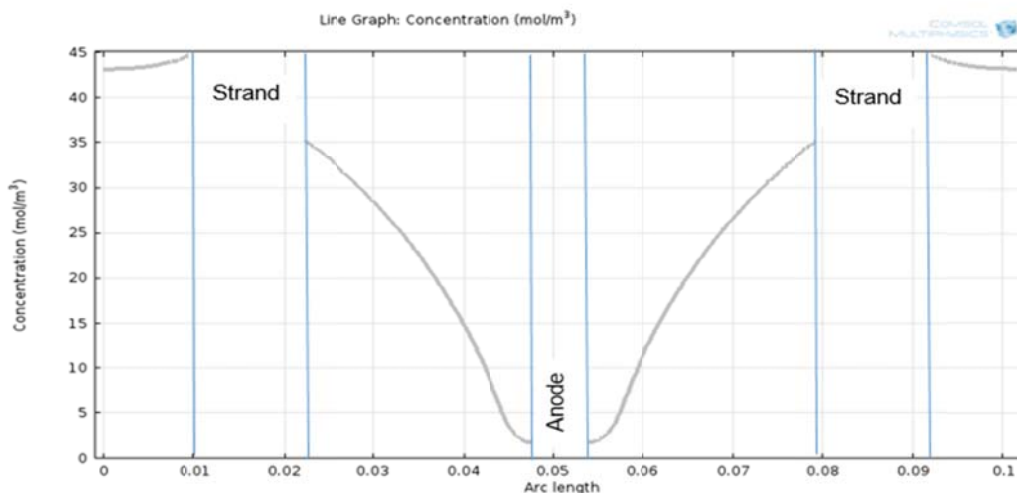


Figure 5: Hydroxide Concentration Versus Distance of a Slice Through the Duct During the Stabilization Period of the Base Case Parameter Set. Note the Concentration Decreases Towards the Central Anode Until it Reaches the Calcium Hydroxide Dissolution Zone Shown in Figure 7 Where it Levels Off.

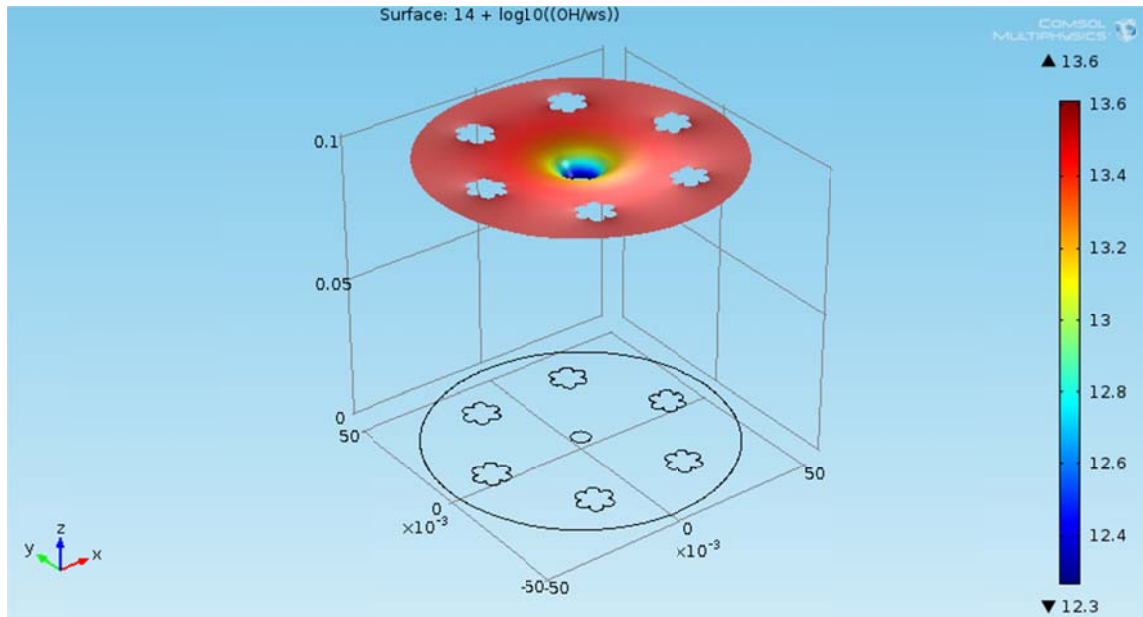


Figure 6: pH Distribution During the Stabilized Period Predicted by the Model's Base Case Parameter Set.

At the anode, the current and therefore rate of hydroxide consumption (Eq. 6) is proportional to the concentration of hydroxide at the surface of the anode (Eq. 5). The depletion of hydroxide at the anode therefore limits the magnitude of the inward current density of the anode to the rate at which hydroxide can be transported to the anode from the cathodes where the reverse reaction is occurring. As the hydroxide concentration near the anode decreases the calcium hydroxide in this region begins to dissolve releasing hydroxide and calcium ions into the pore water and limiting the extent of the depletion of hydroxide at the anode. This effect can be seen in the flattening out of the hydroxide profile near the anode in Figure 5. While calcium hydroxide is still present near the anode this process limits the amount of current reduction due to hydroxide depletion at the anode and protects the anode from acidification.

The model uses a kinetic theory of dissolution to project the rate of calcium hydroxide depletion at the anode. Figure 7 shows the base case parameter set projection of the calcium hydroxide concentration in the grout of a slice through the model passing through the anode every ten years from year 0 to year 100. It is observed that the base case parameter set model output projects roughly 100 years until complete calcium hydroxide depletion at the anode to a depth of 0.2 cm. Figure 8 shows the distribution of calcium hydroxide over the entire surface of the grout after 100 years.

The projected calcium hydroxide depletion is dependent upon the pore water hydroxide concentration, hydroxide diffusivity and the anodic current density. However, for the cases examined in which the polarization and current delivery criteria were satisfied, projected CaOH_2 depletion and anode acidification was moderate enough to indicate that these effects were not an important limitation for system performance during the 100 year interval explored.

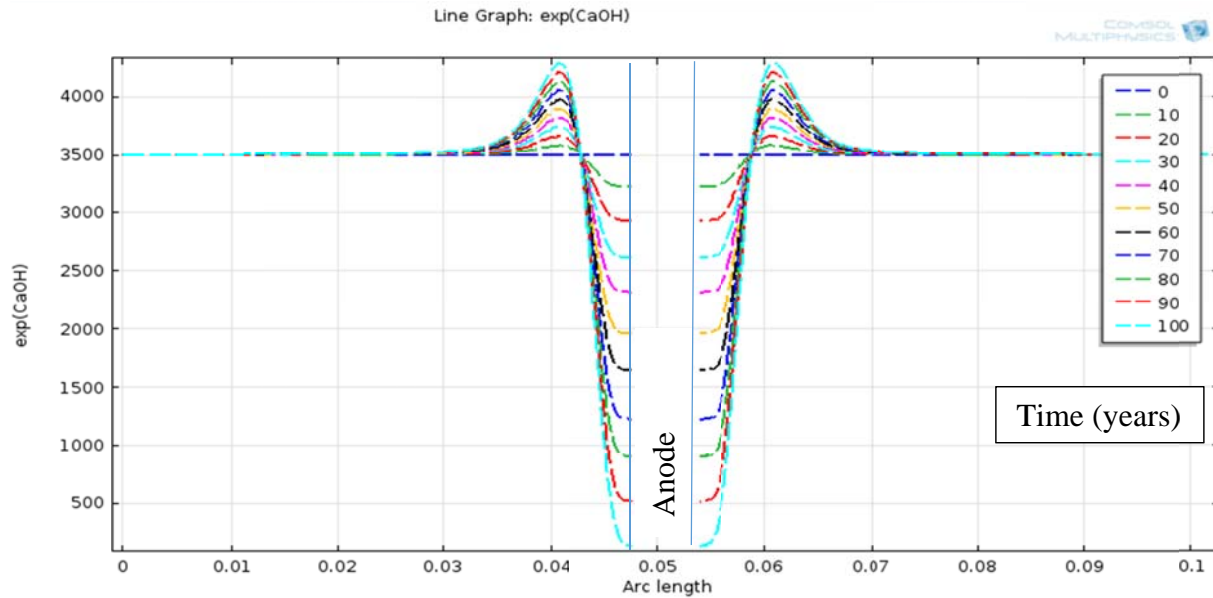


Figure 7: Calcium Hydroxide profile projected by base case parameter set over time in 10 year intervals from year 0 to year 100.

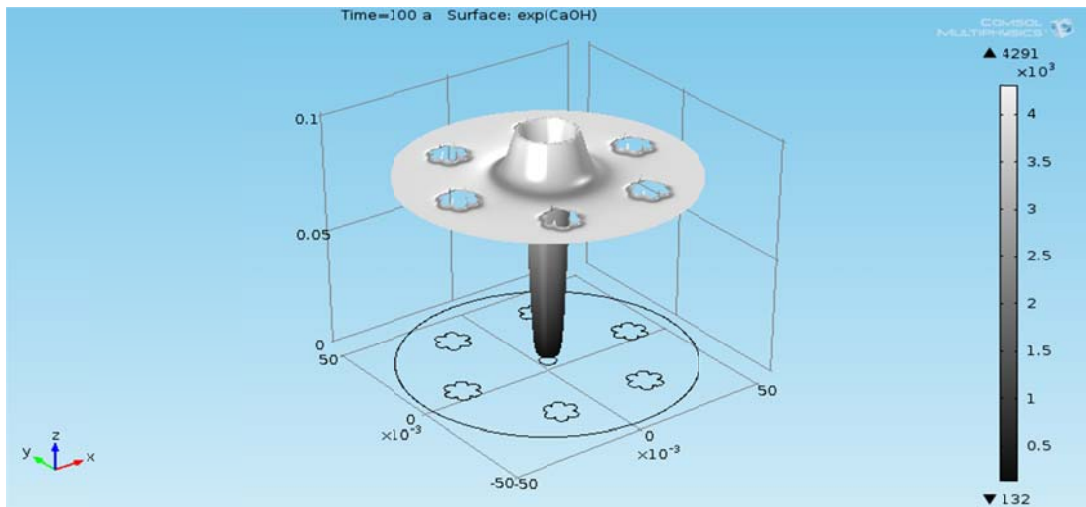


Figure 8: Calcium Hydroxide Depletion Predicted by the Base Case Parameter Set at the Anode After a Period of 100 Years. Scale is in Moles Of Solid CaOH_2 Per m^3 Of Grout.

Anode Size

For the purposes of our calculations a circular cross section anode has been assumed. It may be beneficial from a design perspective to use instead a flat or mesh anode to reduce the total anode material use or to increase the mechanical flexibility of the anode. It is reasonable to assume that a mesh anode or flat strip with a surface area similar to that of a circular anode would have similar electrochemical behavior for the following reasons. First the reactions are happening at the surface of the anode and as such the current density for a given total current is inversely proportional to the total anode surface area. Since the limiting system efficacy conditions (hydroxide depletion and calcium hydroxide dissolution) are primarily dependent upon the current density coming from the anode and the

distance between the anode and cathodes, the effects of these limiting conditions should be relatively independent of shape effects given a similar total anode surface area. Second, if there is no important convective flow (a reasonable assumption in the absence of information to the contrary) it is unlikely that the shape of the anode will significantly affect the delivery of reactive species to the anode's surface.

The initial calculations were done assuming a pre-installed ¼ inch diameter anode running along the space otherwise used for central wire stand. A small anode is desirable from a design perspective as it reduces the cost of the anode material and increases the anode's mechanical flexibility making it easier to work with and avoid short circuits. Increasing the size of the anode will increase its surface area and thereby reduce the current density at the anode for a given total current. A reduction in the anodic current density is desirable from an electrochemical perspective since the local depletion of hydroxide and rate of dissolution of calcium hydroxide at the surface of the anode are both positive functions of the inward current density. Ideally the anode used would be the smallest possible anode large enough to ensure cathodic protection over the lifetime of the system without detrimental changes in the immediately surrounding grout (or other potential complications not investigated here, such as large anodic current densities causing excessive local temperature increase around the anode).

The calculations indicated that an anode of this size would be sufficient to protect the system assumed within the range parameters modeled without requiring excessive current demand from the anode. If, however, the grout resistivity is significantly higher or the pore hydroxide content is significantly lower than what has here been assumed, using a larger anode may be prudent to reduce the current demand of the anode or to increase the time to calcium hydroxide depletion at and acidification of the anode. In this context, the model approach is not limiting and other system dimensions and number of strands could be easily implemented to explore alternative situations.

Hydrogen Evolution

In electrochemical systems with a pH in the range of 13-14 hydrogen evolution is possible under a polarization voltage of -900mV (regular sign convention) versus a standard calomel electrode (SCE)^{5,6}. Evolved hydrogen could diffuse quickly into the steel strand, embrittling the steel, and ultimately causing failure. For this reason, it is important that the potential of the steel strand under cathodic protection does not go significantly beyond the value indicated above. The model projects a strand potential safely distant from this value (for instance a potential of -350 mV [regular sign convention] is projected using the base case parameter set) when CP is applied, as indicated in the assumptions, to non-corroding steel. Since the CP system as simulated here is meant to be implemented when the strands are newly put into place, the non-corroding condition that the steel is assumed to be in would likely be justified. However, further consideration and model expansion will be necessary to examine the likelihood for hydrogen evolution initiation in corroding steel.

FEM Mesh Sensitivity and Current Balance Check

Because of significant sensitivity to distance between nodes in the kinetic model, a very fine maximum node separation distance of 0.0005m was chosen. At this level the model was found to be fairly insensitive to changes in mesh size. Increasing the maximum node separation distance by an order of magnitude to 0.005m (a 99% reduction in node density) was found to increase the minimum stabilized cathodic current in the base parameter set by only 12%, from 0.88 $\mu A/(cm^2)$ to 0.98 $\mu A/(cm^2)$, so the results are reasonably stable in a compromise between practical use and computational resource/time needs.

Another simple check of model self-consistency is to examine if the total anodic and cathodic currents are equivalent or close to equivalent. If they are not equivalent then the model is predicting net charge buildup, which would violate the principle of net neutrality (equation 8). An integration of the anodic and

cathodic currents showed the current balance to be always within ~2% or better of the total current, indicating the robustness of the approach used here.

CONCLUSIONS

The exploratory model projections suggest that, within the context of the system configuration assumed and tentative selection of parameters values used, an impressed current cathodic protection system installed internally into a grouted duct for the purpose of cathodic protection of steel tensioning strand may be feasible (for the case of initially passive steel). In particular:

1. The projected minimum cathodic current attainable was in the range typical of cathodic protection systems over a wide range of grout resistivities
2. The projected steel potential shift for a cathodic current typical of cathodic protection systems met a typical criterion for cathodic protection systems.
3. At steel polarization shift levels typical of cathodic protection systems the projected steel polarization did not reach a level that would initiate Hydrogen evolution (if the steel was not corroding prior to system polarization).
4. At current levels typical of cathodic protection, projected anode acidification was slow enough that it would not appear to promote appreciable performance deterioration over a 100 year design lifetime.

The calculations presented here are initial and exploratory in nature. Given the significant simplifying assumptions of the model and limitations of modelling in describing real world electrochemical phenomena, empirical validations of the model's projections will be critical in validating the model's veracity. The more demanding case of polarization of actively corroding steel should be evaluated in follow up work.

ACKNOWLEDGEMENTS

This work was done with the support of the Florida Department of Transportation, and in particular Ivan Lasa. The opinions, findings, and conclusions expressed in this publication are those of the authors and not necessarily those of the State of Florida Department of Transportation.

REFERENCES

1. Lee, S.K. and Krauss, P.D. "Long-Term Performance of Epoxy-Coated Reinforcing Steel in Heavy Salt-Contaminated Concrete," Federal Highway Administration Report FHWA-HRT-04-090, 2004.
2. G.H. Koch, M.P.H. Brongers, N.G. Thompson, Y.P. Virmani, and J.H. Payer, "Corrosion Costs and Preventive Strategies in the U.S.," FHWA-RD-01-156, Federal Highway Administration, Washington, D.C., 2002
3. Bartholomew, J., Bennett, J., Turk, T., Hartt, W. H., Lankard, D. R., Sagüés, A. A., Savinell, R., "Control Criteria and Materials Performance Studies for Cathodic Protection of Reinforced Concrete," Strategic Highway Research Program, National Academy of Sciences, Washington D.C., 1993.
4. Rafols, J.C., Lau, K., Lasa, I., Paredes, M. and Elsafty, A. "Approach to Determine Corrosion Propensity in Post-Tensioned Tendons with Deficient Grout." OJCE Open Journal of Civil Engineering, Volume 3, p 182-187, 2013.

5. Enos, D. G., Williams, A. J., and Scully, J. R. "Long-Term Effects of Cathodic Protection on Prestressed Concrete Structures: Hydrogen Embrittlement of Prestressing Steel", *Corrosion*, 53, p 891-908,1997.
6. Hartt, W. H., Kumria, C.C., and Kessler, R.J., "Influence of Potential, Chlorides, pH, and Precharging Time on Embrittlement of Cathodically Polarized Prestressing Steel", *Corrosion*, 49, p. 377-385,1993.
7. Peelen, W., Larbi, J., Polder, R., E. Redaelli, L. Bertolini, "Qualitative model of concrete acidification due to cathodic protection," *Materials and Corrosion*, Volume 59, p 81-89, 2008.
8. Newman, J., & Alyea, K., *Electrochemical systems*, 3rd ed. Hoboken, N.J., 2004.
9. Dugarte, M.. "Polarization of Galvanic Point Anodes for Corrosion Prevention in Reinforced Concrete." Dissertation, University of South Florida, April 2' 2010.
10. Sagüés, A.A., Pech-Canul, M..A. and Al-Mansur, S., *Corrosion Science*, 45, p.7-32, 2003.
11. Ukrainczyk, N., Koenders, E. and Breugel, K., "Numerical Model for Multi-Ion Diffusion in Cementitious Materials – MultiDiff Code," *Matrib*, 07/2013.
12. Shehata, M. H., Thomas, M. D. A., and Bleszynski, R. F. "The effects of fly ash composition on the chemistry of pore solution in hydrated cement pastes," *Cement and Concrete Research*, 29, p. 1915–1920, 1999.
13. Diamond, S., "Effects of two Danish flyashes on alkali contents of pore solutions of cement-flyash pastes", *Cement and Concrete Research*, 11, p. 383-394, 1981.
14. Marchand, J., Bentz, D.P., Samson, E., and Maltais, Y. "Influence of Calcium Hydroxide Dissolution on the Transport Properties of Hydrated Cement Systems," *Materials Science of Concrete: Calcium Hydroxide in Concrete*, American Ceramic Society, Westerville, p. 113. 2001.
15. Chen, W., Brouwers, H. J. H., "A Method for Predicting the Alkali Concentrations in Pore Solution of Hydrated Slag Cement Paste," *Journal of Material Science*, 46, p. 3622 – 3631, 2011.
16. Truc, O., Ollivier, J., and Nilsson, L., "Numerical simulation of multi-species transport through saturated concrete during a migration test — *MsDiff* code," *Cement and Concrete Research*, 43, p 1581 – 1592, 2000.
17. Kranc, S.C. and Sagüés, A.A., "Calculation of Extended Counter Electrode Polarization Effects on the Electrochemical Impedance Response of Steel in Concrete," *Electrochemical Impedance: Analysis and Interpretation*, ASTM STP 1188, American Society for Testing and Materials, Philadelphia, 1993, p. 365-383.
18. Glass, G. and Chadwick, J., "An Investigation into the Mechanisms of Protection Afforded by a Cathodic Current and the Implication for Advances in the Field of Cathodic Protection", *Corrosion Science*, 36, p. 2193-2209, 1994.
19. Jones, D. A., "Principles and Prevention of Corrosion", 2nd edition, Prentice- Hall, Inc., 1996.
20. Funahashi, M. and Bushman, J. B. "Technical Review of 100 mV Polarization Shift Criterion for Reinforcing Steel in Concrete," *Corrosion*, 47, p. 376-386, 1991.